Evaluation of MACRO model by short-term water and solute transport simulation in Maury silt loam soil

H. Merdun[1], V.L. Quisenberry[2]

[1]*Faculty of Agriculture, Kahramanmaraş Sütçü Imam University, Turkey*
[2]*Faculty of Agriculture, Clemson University, USA*

ABSTRACT

Modeling preferential flow has been a concern of many academic fields in the past 30 years all over the world and helps to prevent groundwater contamination. A dual-porosity model, MACRO, was evaluated for short-term (less than 2 days) simulation of water flow and non-reactive solute (chloride) transport through the profile of six plots in well-structured Maury silt loam soil. Water flow in micropores is calculated by the Richards' equation while simple gravity flow is assumed in the macropores. Solute transport in the micropores is calculated by the convection-dispersion equation (CDE) while the dispersion and diffusion in the CDE is neglected for the solute transport in the macropores. The applied water and chloride reached the bottom of the profile during the 2 and 1-hour(s) application periods in studies 2 and 3, respectively. There is a strong indication of macropore flow in this soil. Based on the statistical criteria, the model accurately simulated water flow and solute transport with depth and time in all plots. The mean values of three statistical parameters (coefficient of residual mass, model efficiency, and correlation coefficient) for water and chloride transport were –0.0014, 0.791, 0.903 and 0.0333, 0.923, 0.956, respectively. Preliminary studies showed that the model could not simulate flow and transport well enough with the one-domain flow concept. In the two-domain flow, effective diffusion path-length, boundary hydraulic conductivity, and boundary soil water pressure were the three most important parameters that control flow and transport between the two domains. The effective diffusion path-length represented the structural development with depth in the Maury silt loam soil.

Keywords: MACRO; macropore flow; modelling; solute transport; structured soil; two-domain

Modelling preferential flow in well-structured soils has been the interest of many academic fields in the past 30 years all over the world to prevent groundwater from contamination. A number of laboratory and field experiments have been conducted to qualitatively describe preferential flow through unsaturated soil and understand the mechanisms that control this type of flow (Quisenberry and Philips 1976, Bouma 1980, Hatfield 1988, Nelson 1990, Flury et al. 1994, Quisenberry et al. 1994, Flury 1996, Sadeghi et al. 2000, Ersahin et al. 2002). Even though many mathematical models have been developed to quantitatively describe preferential flow through macroporous soils (van Genuchten and Cleary 1976, Skopp et al. 1981, Chen and Wagenet 1992, Gerke and van Genuchten 1993, Durner 1992, 1994, Hutson and Wagenet 1995, Mohanty et al. 1997, Zurmuhl and Durner 1998), none of them are complete for quantitative description and the incorporation of soil structures into these models. The mobile-immobile region concept of van Genuchten and Cleary (1976) and the application of this concept to a structured soil by Skopp et al. (1981) were two of the earliest attempts to make these deterministic models more realistic by introducing these important soil characteristics into the models. Since the soil structural features affect the transport of water and solute, mathematical models of soil transport processes require the relationship between the structural characteristics of the soil and these transport equations (Quisenberry et al. 1994).

In mobile-immobile region concept models, the pore system in well-aggregated natural soils, like Maury silt loam, is frequently divided into two domains: micropores (intraaggregate pores) and macropores (interaggregate pores) and each domain has its own water content, conductivity, and flux (Gerke and van Genuchten 1993, Zurmuhl and Durner 1998). These models have shown promising results for the simulation of flow and transport at the soil column or monolith (Jarvis et al. 1994, Saxena et al. 1994), but only a few of these models have been tested or evaluated for field conditions due to the lack of the measured data.

One of these models is MACRO (Jarvis and Larsson 1998), a complex physical model for the simulation of flow and reactive and non-reactive chemicals with consideration of shrinkage. The main advantage of modelling is the testing theory or devising new management strategies. Validated models can be useful to understand complex flow and transport processes in the unsaturated zone. The MACRO model has been tested or evaluated by several researchers for different types of field soils and durations (Jarvis et al. 1991a, b, Andreu et al. 1994, Jabro et al. 1994, Saxena et al. 1994, Jarvis 1995, Villholth and Jensen 1998, Jarvis et al. 1999, Larsson and Jarvis 1999a, b, Armstrong et al. 2000, Gottesburen et al. 2000, Jarvis et al. 2000, Roulier and Jarvis 2003a, b). In these modelling efforts, the model has been tested or evaluated for the long-term simulation of water flow and/or solute and/or pesticide transport under different types of field soils. However, the performance of the model has not been evaluated, as far as our knowledge, for the short-term simulation of flow and transport under field conditions.

Therefore, the objective of this study is to evaluate the ability of the MACRO model by simulating water flow and solute (chloride) transport in the profile of six plots of Maury silt loam, a well-structured soil, during a short-time period (less than 2 days) and define critical processes and model parameters governing macropore flow. The model predictions were compared with the measurements of water content and chloride concentration with depth and time to satisfy these objectives.

MODEL DESCRIPTION

MACRO model (Jarvis and Larsson 1998) is a detailed mechanistic dual-porosity model of water and solute transport in a macroporous soil. The model is a non-steady state simulation of water flow and solute transport in a one-dimensional (vertical) heterogeneous-layered field soils. A complete water balance is considered in the model, including saturated and unsaturated water flow, canopy interception and root water uptake, and seepage to drains and groundwater. The model can be used to simulate non-reactive tracers (bromide, chloride), tritium, and pesticide transport.

One of the important features of the model is that it can be run in either one (micropore) or two flow domains (micropore + macropore) using the same soil hydraulic properties. This feature of the model helps to evaluate the impact of preferential water flow and solute transport on surface and groundwater in structured soils quantitatively. In the two-domain flow, the total soil porosity in each layer in the profile is divided into two flow regions, micropores and macropores, where each of them has their own water content, hydraulic conductivity, and flux. The interaction of the two regions is represented by a first order kinetic equation. In the one-domain case, the model reduces to the Richards' and convection-dispersion equations (Richards 1931). The model requires climatic data and physical/hydraulic parameters as input. Since the model is presented in detail elsewhere (Jarvis and Larsson 1998), we will only describe in detail the parts that are especially related to this study.

Flow and transport equations

The soil porosity is divided into two domains, micropores and macropores, at a given soil water pressure (ψ_b) and corresponding water content (θ_b) and hydraulic conductivity (K_b). Micropores and macropores act as separate flow regions and each characterized by a degree of saturation, conductivity, and flux. The vertical water flow through the micropores in the unsaturated zone is calculated using the Richards' equation:

$$\frac{\partial\theta}{\partial t} = -\frac{\partial}{\partial z}\left[K_{mi}\left(\frac{\partial\psi}{\partial z}+1\right)\right] \pm S_w \qquad (1)$$

where: θ is the water content, K_{mi} is the unsaturated hydraulic conductivity in the micropores, ψ is the soil water pressure, t is time, z is vertical distance, and S_w accounts for water exchange between the two domains. The water release characteristic, $\psi(\theta)$, and the hydraulic conductivity function in the micropores, $K(\theta)$, are calculated by the Brooks and Corey (1964) and the Mualem (1976)'s equations, respectively:

$$\psi_{mi} = \psi_b\left(\frac{\theta-\theta_r}{\theta_b-\theta_r}\right)^{-\frac{1}{\lambda}} \qquad (2)$$

$$K_{mi} = K_b\left(\frac{\theta-\theta_r}{\theta_b-\theta_r}\right)^{n+2+2/\lambda} \qquad (3)$$

where: θ_r is the residual soil water content in the micropores, θ_b is the boundary water content (the saturated water content in the micropores), ψ_b is the boundary soil water pressure (the pressure at the boundary water content), λ is the pore-size distribution index in the micropores, K_b is the boundary hydraulic conductivity (the saturated hydraulic conductivity in the micropores), and n is the tortuosity factor in the micropores.

The vertical water flow through the macropores is calculated by the Darcy's equation assuming a unit hydraulic gradient (laminar flow under gravity, that is, tension is not considered). This approach is numerically equivalent of the analytical kinematic wave model (Beven and Germann 1982). The unsaturated hydraulic conductivity in the macropores, K_{ma}, is calculated by a simple power-law function of the degree of saturation (Beven and Germann 1981):

$$K_{ma} = K_b + (K_s - K_b)\left(\frac{\theta - \theta_b}{\theta_s - \theta_b}\right)^{n^*} \quad (4)$$

where: K_s is the saturated hydraulic conductivity in the whole domain, θ_s is the saturated water content, and n^* is the tortuosity factor in the macropores.

Water exchange between the two domains, S_w, is treated as an approximate first-order process, neglecting the influence of gravity and assuming a rectangular-slab geometry for the aggregates (van Genuchten and Dalton 1986):

$$S_w = \left(\frac{3D_w \gamma_w}{d^2}\right)(\theta_b - \theta_{mi}) \quad (5)$$

where: D_w is the effective water diffusivity, γ_w is the scaling factor introduced to match the approximate and exact solutions to the diffusion problem (Gerke and van Genuchten 1993), d is the effective diffusion pathlength (i.e. half the aggregate width), and θ_{mi} is the water content in micropores. Because the scaling factor does not vary much with the initial water content and hydraulic properties (Gerke and van Genuchten 1993), it is set to an average value of 0.8 in the model.

Solute transport in the micropores is calculated by the convection-dispersion equation (CDE):

$$\frac{\partial(\theta c)}{\partial t} = \frac{\partial}{\partial z}\left(D\theta \frac{\partial c}{\partial z} - qc\right) \pm U_e \quad (6)$$

$$D = D_v \nu_{mi} + D_0 f^* \quad (7)$$

where: c is the solute concentration, D is the dispersion coefficient, D_v is the dispersivity, D_0 is the diffusion coefficient in free water, v_{mi} is the pore water velocity, f^* is the impedance factor (the constant), q is the Darcy water flux density, and U_e is the mass exchange between flow domains, respectively.

The solute transport in the macropores is calculated by neglecting the dispersion and diffusion in the CDE so that convective transport is a dominant process in the macropores. The diffusive exchange of solute between the two flow domains and the convective fluxes of water and solute into the micropores are considered in the model. The exchange rate of solute between the micropores and macropores, U_e, is calculated by a combination of diffusion and convection (Jarvis and Larsson 1998).

Boundary conditions

The boundary condition at the soil surface is very important in the two-domain model because it controls the partitioning of precipitation between macropores and micropores (Beven and German 1981). The model routes water into surface-vented macropores if the rainfall intensity exceeds the saturated hydraulic conductivity in micropores and soil water pressure is greater than the pressure at saturation at the soil surface. The surface boundary condition is chosen not to have over-saturation in the micropores and partitions the net precipitation R into an amount taken up by micropores (I_{mi}) and an excess amount flowing into macropores (I_{ma}). These conditions are expressed mathematically in the model as:

$$I_{mi} = R,\ I_{ma} = 0 \text{ for } R =< I_{\max} \quad (8)$$

$$I_{mi} = I_{\max},\ I_{ma} = R - I_{mi} \text{ for } R > I_{\max} \quad (9)$$

where: $I_{\max}$ is the infiltration capacity of the micropores.

The model has five options to describe the bottom boundary condition for water flow: constant hydraulic gradient, zero flux, constant pressure head, a water table in the profile, and a lysimeter with free drainage. A lysimeter with free drainage was used in our studies as bottom boundary condition.

MATERIAL AND METHODS

Field data for the study

Quisenberry and Philips (1976) conducted three experimental studies on the Maury silt loam soil in Kentucky to study percolation of surface-applied chloride-tagged water under field conditions. The top 90 cm of the profile at the experimental site may be described as follows: dark brown, very friable silt loam with moderate granular structure at the surface 30 cm and reddish brown, friable, silty clay loam with moderate blocky structure between thirty and 90 cm. The Maury silt loam site was under bluegrass (*Poa pratensis*) for 5 years, but the grass was clipped very close to the soil surface before the initiation of the experiments. Six plots (two plots for each study) on a nearly level land (0–1% slope) were prepared by enclosing an area of 213 cm square by boards placed 5 cm into the soil to prevent runoff and lateral movement of water from the plot area.

Water-tagged chloride, with the application rate and concentration of 4.14 cm/2 h and 4610 μl/L for the studies 1 and 2 and 2.16 cm/1 h and 5849 μl/L for the study 3, was applied to the surface of each plot by hand with a wide-nozzle garden hose. The water flowed by gravity from an elevated barrel, as a result, the rainfall intensity decreased slightly with time as the water head decreased. The application rates were approximately the same (4.14 cm/2 h for the studies 1 and 2 and 2.16 cm/1 h for the study 3) for three studies. Ponding was never observed in any of the plots. The distribution of water content and chloride concentration was measured periodically from immediately after water application ceased until approximately 30 hours later with depth (13 layers) in 90-cm profile using the samples collected at the desired depths with a 2 cm diameter auger soil sampler. The details on the frequency of measurements and depths of sampled layers are given in the Results and Discussion section. Additionally, the initial water content and chloride concentration, bulk density, and field capacity were measured for each plot. The major difference among the three studies was the initial water content to determine the effect of the initial water content on water flow and solute transport in this well-structured soil. The initial water contents of the studies 1 and 2 were similar in the surface 40 cm, whereas the initial water content of the study 2, conducted 5 m away from the study 1, and was approximately 5% greater than that of the study 1 below the 40 cm. The study 3 had higher initial water content throughout the profile. Table 1 gives the particle size distribution with depth for Maury silt loam soil (for the site and experimental details see Quisenberry and Philips 1976).

Table 1. Particle size distribution with depth in Maury silt loam

Depth interval (cm)	Particle size distribution (%)		
	sand	silt	clay
0–5	6.0	68.6	25.4
5–10	5.4	68.3	26.3
10–15	5.5	69.2	25.3
15–22	4.7	65.2	30.1
22–30	6.0	63.0	31.0
30–38	6.4	56.2	37.4
38–45	7.4	54.9	37.7
45–60	6.9	47.2	45.9
60–75	7.5	41.1	51.4
75–90	6.7	37.4	55.9

Sensitivity analysis of the MACRO model

Sensitivity analysis is the testing of the response of model output to variations in selected input parameters. Sensitivity analysis helps to determine the relative sensitivity of the output to changes in input parameters of the model. The identification of sensitive parameters helps us in selecting the most appropriate parameters for model calibration. The parameters, which are critical to the flow and transport processes and have little experimental information, were selected as input parameters for the sensitivity analysis so that reasonable estimation could be made for the calibration process. The output parameters in the sensitivity analysis were the water content for the soil hydraulic parameters used in the model and chloride concentration for the solute transport parameters at the 7^{th} layer of the profile for 3 h (including 2 h application) simulation of 4.14 cm chloride-tagged water (4610 μl/L).

Model parameterization

Input parameters used in MACRO model simulations may be divided into three groups: those parameters obtained from direct measurements, the parameters obtained from general knowledge or literature sources, and those that are directly calibrated by a comparison of simulated and measured state variables. The parameters that were directly measured were: soil water retention data; hydraulic conductivity as a function of water content; initial soil volumetric water content and solute concentration; bulk density; saturated water content; the day, number, amount, beginning and end of irrigation (actually user defined); and solute concentration in irrigation water. The parameters that was either known or estimated from the literature were: initial soil temperature, excluded volumetric water content, and diffusion coefficient in free water. Effective diffusion pathlength (or aggregate half-width) was inferred from physical properties (particle size distribution) of soil and literature values (Villholth and Jensen 1998, Larsson and Jarvis 1999a, b, Roulier and Jarvis 2003a, b). Saturated hydraulic conductivity was estimated from the report of Romkens et al. (1985). The parameters that were directly calibrated by a comparison of simulated and measured state variables were: boundary hydraulic conductivity, tortuosity factors in macropores and micropores, dispersivity, and mixing depth. In addition, the parameters of boundary pressure potential, boundary water content, residual water content, and pore size distribution index in micropores were derived by fitting model functions to measured soil hydraulic properties.

Since soil water retention data was not measured in the study of Quisenberry and Philips (1976), it was obtained by the modification of the measured data of Romkens et al. (1985) based on the saturated water content and field capacity. When water content is larger than the boundary water content, the pressure is calculated assuming a linear function

$$\psi = \psi_b[(\theta_s - \theta)/(\theta_s - \theta_b)] \quad (10)$$

When the water content is smaller than the boundary water content, the pressure is calculated with the Brooks and Corey (1964) function

$$\psi = \psi_b[(\theta - \theta_r)/(\theta_b - \theta_r)]^{-1/\lambda} \quad (11)$$

After the boundary pressure potential and corresponding water content were estimated visually from the water retention curve for each layer, water-retention was fitted to the data in MATLAB by using the Brooks and Corey (1964) equation (11) to obtain the values of residual water content and the pore size distribution index in the micropores. If the water-retention data was not fitted accurately, a different boundary soil water pressure and corresponding water content was chosen from water-retention curve until the retention data was fitted.

When water content was larger than the boundary water content, a simple power law function

$$K = K_b + (K_s - K_b)[(\theta - \theta_b)/(\theta_s - \theta_b)]^{n^*} \quad (12)$$

was used to fit measured conductivity-water content relationship. The tortuosity factors in macropores, n^*, and micropores, n, were used as fitting parameters.

After the simulation of water content with depth and time in each plot, the measured chloride distribution was simulated. Three parameters affected solute transport in the model: 1) excluded volumetric water content, 2) dispersivity, and 3) mixing depth. Excluded volumetric water content due to anion exclusion was not measured for the site, but it was mostly assumed to be zero in the literature. Besides, Thomas and Swoboda's (1970) determination excluded volumetric water content as less than 4 and 6% for Amarillo sandy loam and Llano Vermiculite soils from Llano and Hale Counties in Texas, respectively. Therefore, we assumed no anion exclusion in the profile. The dispersivity and mixing depth were directly calibrated by fitting the model's prediction to the observed data. The diffusion coefficient in free water was set to $4.6e^{-10}$ m^2/s from literature for each plot.

Model evaluation

The performance of the model for the simulation of the measured water and chloride distribution was evaluated using both the graphical displays of measured and model results and statistics. The statistics tool (coefficient of residual mass, *CRM*, and model efficiency, *EF*) developed by Loague and Green (1991) were used in this study and can be described as:

$$CRM = \frac{\sum_{i=1}^{N}(P_i - O_i)}{\sum_{i=1}^{N} O_i} \quad (13)$$

$$EF = \frac{\sum_{i=1}^{N}(O_i - \bar{O})^2 - \sum_{i=1}^{N}(P_i - O_i)^2}{\sum_{i=1}^{N}(O_i - \bar{O})^2} \quad (14)$$

where: P_i and O_i are predicted and observed values of water or chloride for the i^{th} layer respectively, and $\bar{O}$ is the mean of the observed values. If the total amount of water or chloride from the model is equal to the measured amount, *CRM* is zero. Negative or positive values of *CRM* indicate the under-prediction or over-prediction of the measured data, respectively. The maximum and ideal value of *EF* is 1.0, while a negative value of *EF* is an indication of a poor fit. In addition, model values are regressed versus measured data and correlation coefficient, R^2, is used to determine the goodness-of-fit.

RESULTS AND DISCUSSION

Even though water and chloride distribution in the profiles of six plots (two for each study) at different times following the application were simulated in this study, the results of the first plot of each study are presented graphically in Figures 1–3. However, the percent recovery of applied chloride-tagged water and statistical evaluation of the model performance at different times for three percolation studies are given in Table 2. An application of 4.2 cm of chloride-tagged water in both the field and model increased the water content and chloride concentration to the 90 cm depth within 1 h following the application even though the volumetric water content was 5% below the field capacity through the profile of plot 1 of the first study (Figure 1). Although the applied water and chloride was recovered by the model completely in the profile all times following the application, the measured water and especially chloride were lost from the profile at corresponding times (Table 2). The applied water and chloride could not be recovered by the measurement and model in the profile of plot 2 of the first study at all times.

In the second study conducted at a slightly higher initial water content, the results revealed that 20% of a 4.2 cm applied water penetrated below 90 cm immediately after application, and 40% penetrated below 90 cm within 1 h in plot 1 (Figure 2). A great amount of water and chloride could not be recovered by the measurement and model with time in the profiles of plots 1 and 2 of the second study (Table 2).

The results of study 3 also revealed that a large percentage of the applied water moved below 90 cm in a short period of time. Measured and model water and chloride also reached the bottom of the profile of plot 1 during the 1 h application period (Figure 3). Although measured water content de-

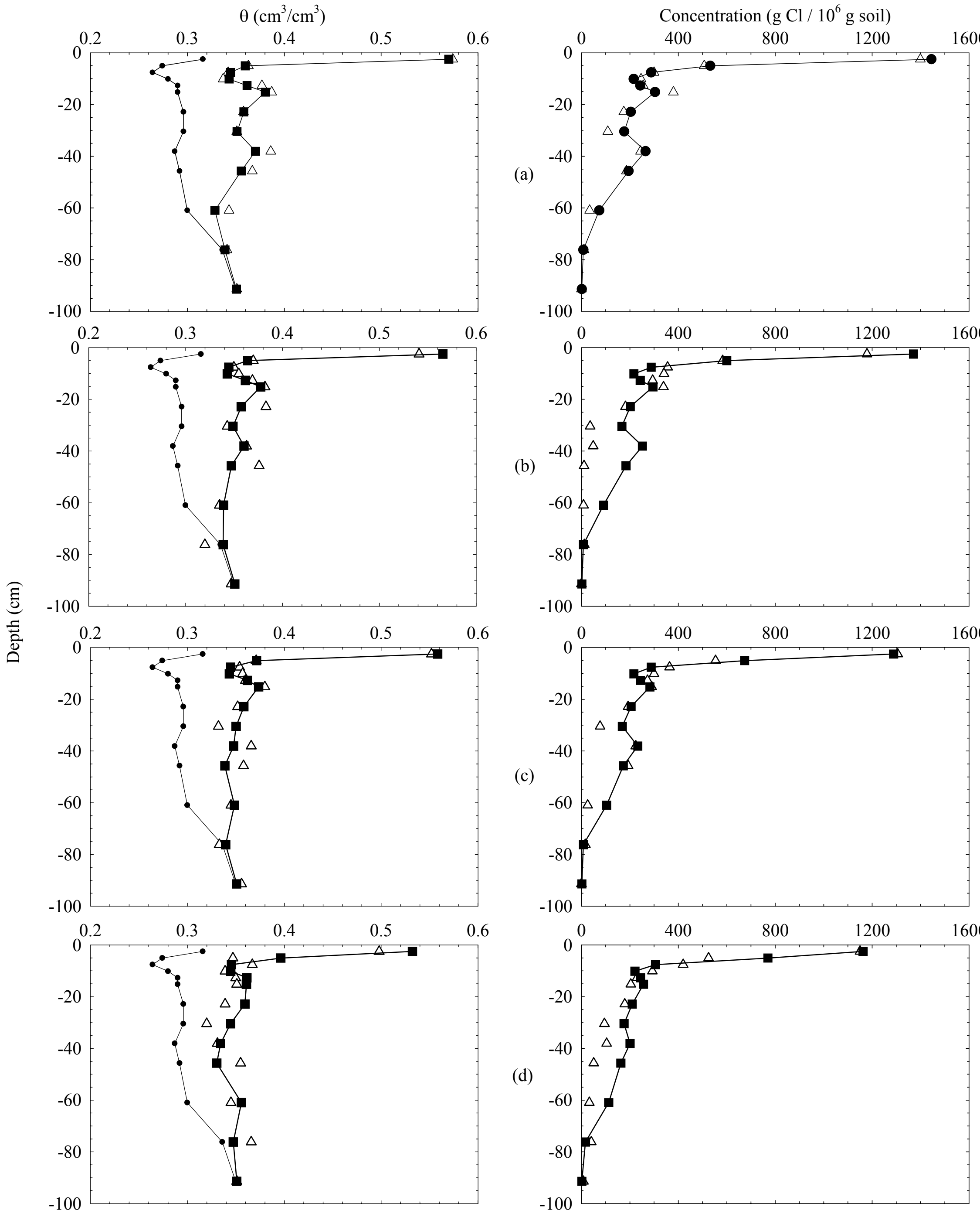

Figure 1. Measured (triangle) and model (square) soil water content (left) and measured (triangle) and model (square) chloride concentration (right) with depth at the times of (a) 1, (b) 3, (c) 7, and (d) 31 hour(s) after the application ceased in the plot 1 of study 1; the third line (circle) refers to the initial water content

creased from 110 to 22% within 24 hours following the application in plot 1, the model recovered 90 and 54% of applied water at the corresponding times (Table 2). This is a strong indication of preferential flow in this soil.

Figures 1–3 show that the relative increase in chloride with depth corresponds very well with the increase in water content. This indicates that the increase in water content throughout the profile was due to the applied water moving through the profile and not displacing the initial water. If the relative increase in chloride did not correspond to the increase in water content, the displacement of antecedent soil moisture in the soil matrix with the applied water would be relatively high (Quisenberry and Philips 1976). Quisenberry and Phillips (1976) calculated the displacement as 3 and 15% for two studies in Maury silt loam soil.

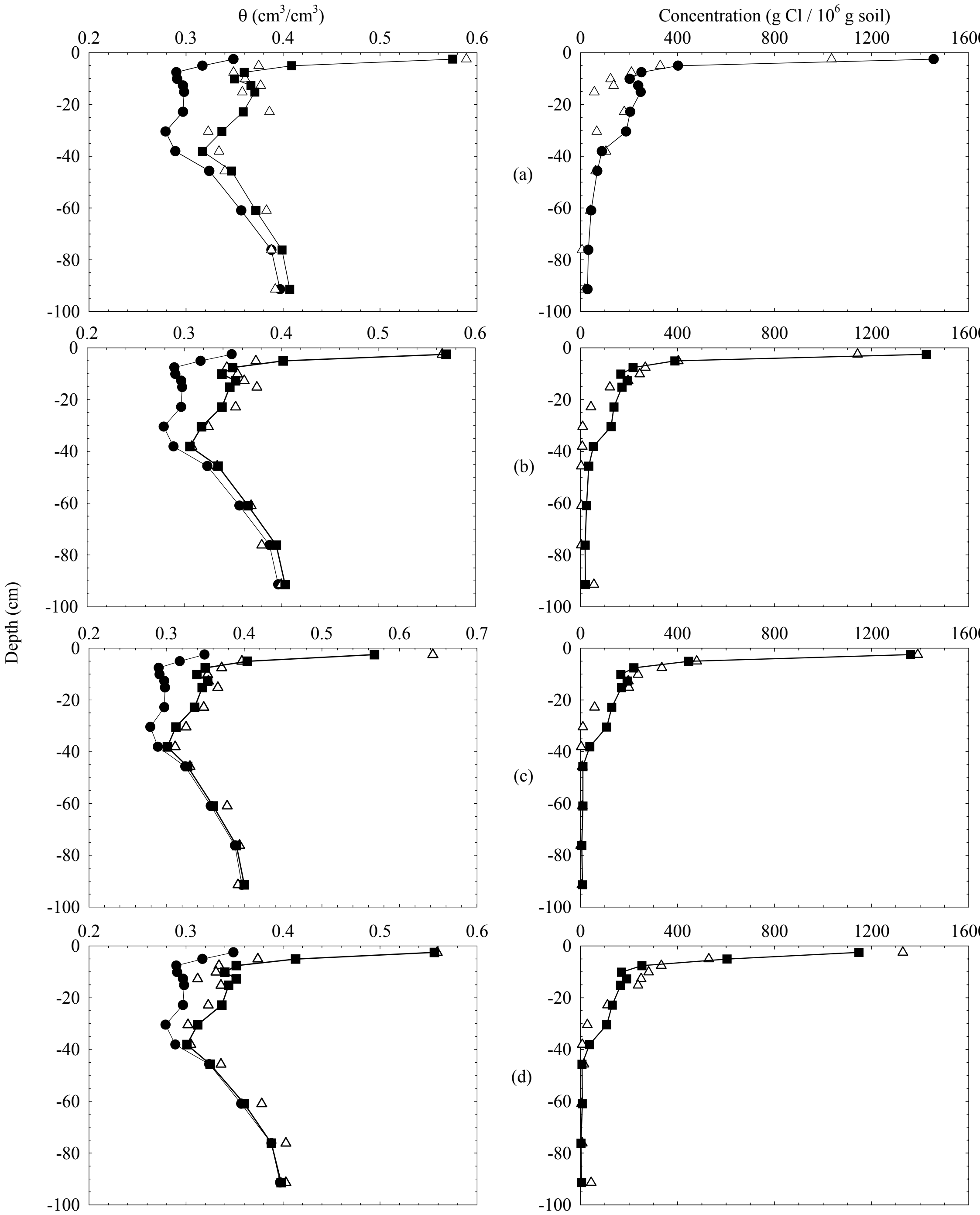

Figure 2. Measured (triangle) and model (square) soil water content (left) and measured (triangle) and model (square) chloride concentration (right) with depth at the times of (a) 0, (b) 1, (c) 6, and (d) 38 hour(s) after the application ceased in the plot 1 of study 2; the third line (circle) refers to the initial water content

This indicates that the applied water displaces little of the initial water during percolation. If there were a 100% displacement of applied water with the antecedent soil water, chloride-tagged water would reach the depth of about 4.5 cm (4–5 cm) and would not be distributed throughout the profile. The increase in water content representing the increase in chloride concentration in all studies strongly indicates that little displacement occurred in the profile during percolation of the applied water.

The differences in soil water percolation for the three studies might be attributed to the initial water content profiles in relationship to the field capacity. Study 1 retained approximately 100% of the applied water throughout the initial 24 hours; whereas study 2 lost a significant amount within 1 h. A smaller application in study 3 with a higher

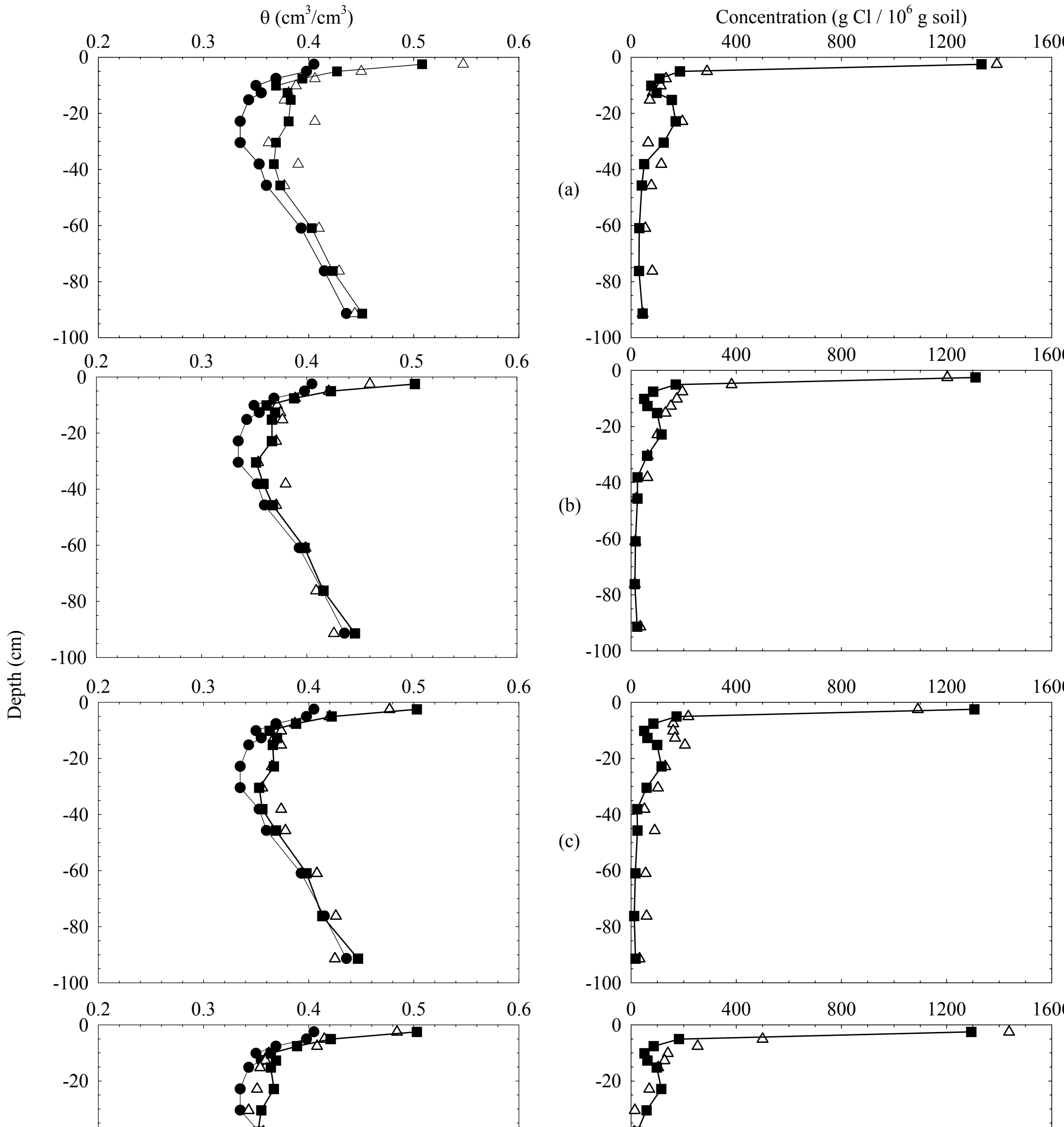

Figure 3. Measured (triangle) and model (square) soil water content (left) and measured (triangle) and model (square) chloride concentration (right) with depth at the times of (a) 0, (b) 2, (c) 8, and (d) 24 hour(s) after the application ceased in the plot 1 of study 3; the third line (circle) refers to the initial water content

initial water content in relationship to field capacity resulted in nearly 50% loss in 2 hours from the 90 cm profile. These results strongly indicate that water can readily pass through the soil even when the soil water content is significantly below field capacity (Quisenberry and Philips 1976).

Results of the model performance analysis are presented in Table 2. Although the model under-predicts ($CRM < 0$) the measured water 52% of the time in all plots, it under-predicts the measured chloride in 38% of the time. The model could not simulate water distribution 8 hours following the application in plot 2 of the third study because $EF < 0$. The 25% of the correlation coefficients, R^2, between measured and model water and chloride in the profiles of all plots for different times are above 0.90 (Table 2). In general, the model predicts water and chloride distribution in the profiles of

Table 2. The percent recovery of applied chloride-tagged water and evaluation of the model performance at different times for three percolation studies on Maury silt loam

				Hours following application					
				1	3	5	7	20	31
Plot 1 Study 1	% recovery	water	measured	111	103	98	98	100	82
			model	100	100	100	100	100	100
		chloride	measured	94	64	77	88	57	74
			model	100	100	100	100	100	100
	evaluation	water	*CRM*	–0.013	–0.007	0.011	–0.006	–0.011	0.023
			EF	0.980	0.921	0.844	0.960	0.896	0.720
			R^2	0.987	0.943	0.944	0.965	0.912	0.836
		chloride	*CRM*	0.028	0.156	0.063	0.020	0.183	0.153
			EF	0.989	0.881	0.943	0.969	0.900	0.898
			R^2	0.990	0.910	0.947	0.970	0.928	0.921
				1	3	16	25		
Plot 2 Study 1	% recovery	water	measured	91	119	96	99		
			model	98	98	98	98		
		chloride	measured	65	80	66	70		
			model	98	98	98	98		
	evaluation	water	*CRM*	–0.017	–0.039	–0.003	0.023		
			EF	0.918	0.926	0.912	0.615		
			R^2	0.933	0.982	0.916	0.726		
		chloride	*CRM*	–0.011	0.008	0.003	0.167		
			EF	0.916	0.921	0.923	0.944		
			R^2	0.925	0.936	0.925	0.959		
				0	1	2	6	28	38
Plot 1 Study 2	% recovery	water	measured	80	60	68	68	62	52
			model	81	60	55	51	49	49
		chloride	measured	54	44	54	44	39	59
			model	83	64	59	56	54	54
	evaluation	water	*CRM*	0.003	–0.004	–0.031	–0.035	0.010	0.018
			EF	0.933	0.949	0.930	0.909	0.875	0.918
			R^2	0.933	0.957	0.964	0.966	0.898	0.928
		chloride	*CRM*	0.458	0.192	–0.049	–0.023	0.150	–0.111
			EF	0.712	0.898	0.922	0.979	0.937	0.953
			R^2	0.971	0.960	0.941	0.980	0.976	0.968
				0.75	1.5	5.5	28	38	
Plot 2 Study 2	% recovery	water	measured	44	42	55	29	24	
			model	57	51	47	46	46	
		chloride	measured	34	40	42	41	32	
			model	60	54	50	50	50	
	evaluation	water	*CRM*	–0.006	0.007	–0.043	0.013	0.025	
			EF	0.944	0.892	0.851	0.892	0.853	
			R^2	0.949	0.925	0.917	0.930	0.888	
		chloride	*CRM*	0.187	0.214	–0.074	0.005	0.106	
			EF	0.933	0.831	0.967	0.967	0.980	
			R^2	0.959	0.937	0.970	0.972	0.986	
				0	2	8	24		
Plot 1 Study 3	% recovery	water	measured	110	54	60	22		
			model	90	57	54	54		
		chloride	measured	114	82	104	75		
			model	92	66	64	64		
	evaluation	water	*CRM*	–0.026	0.003	–0.003	0.020		
			EF	0.860	0.712	0.859	0.867		
			R^2	0.925	0.961	0.944	0.914		
		chloride	*CRM*	–0.098	–0.192	–0.190	–0.253		
			EF	0.977	0.922	0.891	0.911		
			R^2	0.981	0.952	0.983	0.939		
				0	2	8	24		
Plot 2 Study 3	% recovery	water	measured	181	66	26	44		
			model	97	73	71	71		
		chloride	measured	166	74	84	68		
			model	98	78	76	76		
	evaluation	water	*CRM*	–0.045	0.027	0.055	0.011		
			EF	0.115	0.517	–0.539	0.911		
			R^2	0.624	0.802	0.697	0.926		
		chloride	*CRM*	–0.154	0.062	0.019	–0.052		
			EF	0.867	0.952	0.963	0.929		
			R^2	0.932	0.959	0.971	0.966		

all plots for different times acceptably well because *EF* is approximately 1.

Quisenberry and Philips (1976) calculated the coefficient of variation of chloride with a depth at 2 and 24 hours following an application of 2.16 cm of chloride-tagged water in study 3. The coefficient of variation increased with increasing depth from the surface to approximately 15 cm and remained relatively constant from 15 to 90 cm. This abrupt change in coefficient of variation at a specific depth was attributed to a change in the nature of the soil pores conducting water. The surface 15 cm of Maury silt loam has a high organic matter content and porosity, hence, water moves somewhat as a front through the soil rapidly. Below the 15 cm water percolates deeper into the profile through isolated channels. Therefore, two different flow phenomena were observed in the Maury soil: Darcy and preferential flow at the top 15 cm-depth and preferential flow below that point.

The values of parameters should be chosen in such a way that they represent these two types of flow phenomena in the profile of Maury silt loam soil. The model represents these flows by using the two-domain flow concept. Based on the concept, all water should flow through micropores for flow to be complete micropore flow (uniform flow) and through macropores for flow to be complete macropore flow. Since both pore systems operate in any field soil, as in our case, the right combination of these two flows is very important for accurate simulation of flow and

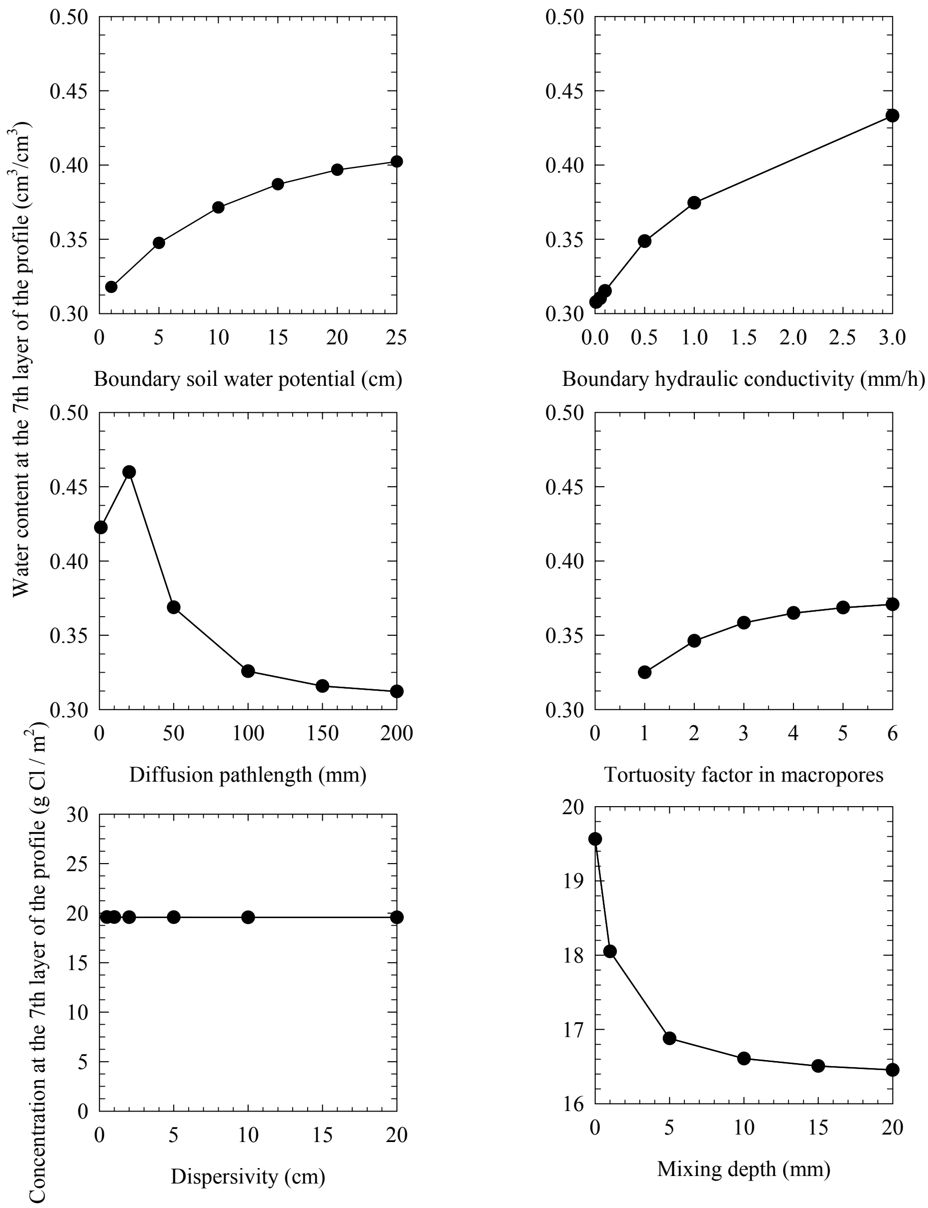

Figure 4. The model sensitivity to physical/hydraulic and solute transport parameters in Maury silt loam

transport. Adjusting or calibrating several model parameters can accomplish the right combination for water and chloride simulations.

The results of the sensitivity analysis are presented in Figure 4. The model seems to be sensitive to the parameters of the effective diffusion pathlength and boundary hydraulic conductivity compared to the parameters of boundary soil water potential, tortuosity factor in macropores, and mixing depth. However, dispersivity is generally insensitively relative to the selected model output.

The soil hydraulic parameters used in the model for the simulation of flow and transport in Maury silt loam soil are presented in Table 3. In MACRO model, the total soil porosity is divided into two regions, micropore and macropore, at a boundary soil water pressure on the water-retention curve. Since there is no certain rule to apply soil to soil to define the division point, this must be done by trial and error to accomplish the simulation. The fitting process should continue until the model and measured water retention data fit. Since the model differentiates soils by the parameters obtained from fitting its soil hydraulic functions (water-retention and conductivity curves), an accurate fit of these functions through the correct values of the boundary soil water pressure and corresponding water content is really critical for acceptable model simulations. The boundary soil water pressure was constant with depth and plot (Table 3). In similar simulation studies, Saxena et al. (1994), Andreu et al. (1994), Jarvis and Larsson (1998), Jarvis et al. (1999), Larsson and Jarvis (1999a), Armstrong et al. (2000), and Roulier and Jarvis (2003b) used the values of –12, –10, –12, –10, –10, –10, and –10 cm (average with depth) for the boundary soil water pressure in long-term studies conducted on a clayey, clayey, clayey, silty clay over clay, clayey, clayey, and clayey soil, respectively, which are pretty close to our value (–7 cm).

Water and chloride move more uniformly above the 15-cm depth due to more uniform distribution of soil pores, but non-uniformity in soil pores (effective soil structure) below that depth causes water to flow rapidly through the macropores. Water might flow either through the micropores, macropores, or the combination of the two. We have explained so far that the boundary values between micropores and macropores control the type of flow. However, the parameter of the effective diffusion pathlength or aggregate half-width also controls the type of flow by exchanging the water between the two domains. The effective diffusion pathlength is one of the most significant parameters in the model because the amount of exchange of water between the two domains is directly related to the inverse square of it (equation 5). The sensitivity analysis of the model also shows the significance of this parameter (Figure 4). Very small values of the effective diffusion pathlength near the surface layers and large values of it for the bottom layers have been set in the model, which transition section takes place between the two regions. The diffusion pathlength varies with depth but constant with plot (Table 3). Similarly, Larsson and Jarvis (1999a) and Armstrong et al. (2000) used the values of 210 and 150 mm (average with depth) for the effective diffusion pathlength in long-term studies conducted on clayey soils,

Table 3. Soil hydraulic parameters used in the model simulations for Maury silt loam

Depth (cm)	ψ_b (cm)	d (mm)	K_s (mm/h)	K_b (mm/h)	λ	θ_s (cm^3/cm^3)	θ_b (cm^3/cm^3)
2.54	7	1	400	0.038	0.372	0.617	0.580
5.08	7	2	300	0.012	0.580	0.553	0.506
7.62	7	5	200	0.033	0.550	0.534	0.486
10.16	7	7.5	150	0.043	0.592	0.522	0.475
12.70	7	7.5	100	0.052	0.585	0.515	0.467
15.24	7	7.5	50	0.055	0.604	0.512	0.461
22.86	7	50	50	0.967	0.618	0.511	0.459
30.48	7	70	50	1.350	0.680	0.508	0.451
38.10	7	100	50	2.733	0.845	0.477	0.445
45.72	7	100	50	2.633	0.884	0.457	0.426
60.96	7	100	50	1.383	0.565	0.441	0.420
76.20	7	100	50	0.652	0.510	0.448	0.430
91.44	7	100	50	0.618	0.274	0.460	0.443

respectively. The larger values of diffusion path-length in their study compared to ours might be expected because soil structural development is more prevalent in a clayey soil.

Because of the high organic matter and porosity, the saturated hydraulic conductivity is very high near the surface. However, since the inter-aggregate pores are mostly effective in the flow processes, relatively smaller values of the conductivity are used for the lower depths. This is supported by the boundary hydraulic conductivity values being very small at the corresponding depths. Since the boundary hydraulic conductivity values are larger at the lower depths, the saturated hydraulic conductivities are smaller. The saturated hydraulic conductivity varies with depth but constant with plot (Table 3). In long-term studies conducted on a clayey, clayey, clayey, clayey, and repellent sandy soil; Saxena et al. (1994), Andreu et al. (1994), and Larsson and Jarvis (1999a, b) used the values in the range of 50–200, 2–300, 5–200, 20–200, and 66–100 mm/h for the saturated hydraulic conductivity, respectively. The large variation of saturated hydraulic conductivity in the profiles of the soils might be the result of the wide range of macropore channels throughout the profile in these soils.

Macropore flow may not occur when the boundary hydraulic conductivity is greater than the application rate. The higher boundary conductivity causes the more micropore flow or less macropore flow. A small increase in the boundary hydraulic conductivity caused the higher retention of water in the profile at earlier times but small changes at later times. The decrease in the boundary hydraulic conductivity forced water to flow through the macropores, therefore, less water was retained in the profile. The mean values of six plots for the boundary hydraulic conductivity with depth are given in Table 3. The small values of boundary hydraulic conductivity (0.01–0.1 mm/h) to a depth of 15 cm and larger values (0.1–10 mm/h) below that point were set in the model. Since the soil structure or inter-aggregate pores below the 15-cm depth was clearly defined, water might readily flow through the macropores. In long-term simulation of water and solute/pesticide transport through the profiles of clayey, sandy, clayey, silt loam, clayey, silty clay over clay, clayey, and clayey soils, Jarvis et al. (1991b), Saxena et al. (1994), Andreu et al. (1994), Jarvis (1995), Jarvis and Larsson (1998), Jarvis et al. (1999), and Armstrong et al. (2000) used the values of 0.05, 0.01, 0.1, 0.1, 0.1, 0.1, 0.1, and 0.05 mm/h (average with depth) for the boundary hydraulic conductivity, respectively, which are similar to our values (Table 3).

The pore size distribution index in the micropores (λ) changes with depth and plot, but the average of the six plots is given in Table 3. Even though there is no clear cut pattern for the distribution of the pore size distribution index, it seems to increase up to the depth of 15 cm and decrease below the 45 cm. Saxena et al. (1994), Andreu et al. (1994), Jarvis (1995), Jarvis and Larsson (1998), Jarvis et al. (1999), Larsson and Jarvis (1999a, b), and Armstrong et al. (2000) used the values of 0.1 and 0.8, 0.04, 0.17, 0.1, 0.05, 0.05, and 0.06 for the pore size distribution index in the micropores in studies conducted on a sandy and clayey, clayey, silt loam, clayey, silty clay over clay, clayey, and clayey soils, respectively.

After the simulation of water content with depth and time in the profile of all plots, the chloride distribution was simulated. We assumed no excluded volumetric water content due to the anion exclusion in the profile of six plots. Roulier and Jarvis (2003b) used the value of 5% for excluded volumetric water content in a soil with similar clay content. Since both the dispersion and the pore water velocity are directly related to the characteristics of the large continuous pores and these characteristics of the pores change from space to space in soils, the value of the dispersivity should change as a function of the space. However, the model allows us to enter the mean value of the dispersivity with the space. The dispersivity was set to 50, 10, 50, 50, 10, and 10 cm for plots 1 through 6, respectively, which is relatively high. The large value of the dispersivity means the more macropore flow or less retention of chloride in the profile. The value of mixing depth affects the solute transport only at the surface depth. The large value of mixing depth means the more displacement of antecedent soil water with the applied water, therefore, the more retention of chloride in the surface layer. The mixing dept was set to 0.0001, 0.001, 0.0000001, 0.0001, 0.8, and 0.6 mm for plots 1 through 6, respectively, which is relatively low.

REFERENCES

Andreu L., Moreno F., Jarvis N.J., Vachaud G. (1994): Application of the model MACRO to water movement and salt leaching in drained and irrigated marsh soils, Marismas, Spain. Agricultural Water Management, *25*: 71–88.

Armstrong A., Aden K., Amraoui N., Diekkruger B., Jarvis N.J., Mouvet C., Nicholls P., Wittwer C. (2000): Comparison of the performance of the pesticide-leaching models on a cracking clay soil: results using the Brimstone Farm dataset. Agricultural Water Management, *44*: 85–104.

Beven K., Germann P. (1981): Water flow in soil macropores II. A combined flow model. Soil Science, *32*: 15–29.

Beven K., Germann P. (1982): Macropores and water flow in soils. Water Resources Research, *18*: 1311–1325.

Bouma J. (1980): Soil morphology and preferential flow along macropores. Agricultural Water Management, *3*: 235–250.

Brooks R.H., Corey A.T. (1964): Hydraulic properties of porous media. Hydrology papers, Colorado State University, Fort Collins, Colorado. No. 3.

Chen C., Wagenet R.J. (1992): Simulation of water and chemicals in macropore soils. Part 1. Representation of the equivalent macropore influence and its effect soil water flow. Journal of Hydrology, *130*: 105–126.

Durner W. (1992): Predicting the unsaturated hydraulic conductivity using multiporosity water retention curves. In: van Genuchten M.Th. et al. (eds.): Indirect methods for estimating the hydraulic properties of unsaturated soils. University of California, Riverside: 185–202.

Durner W. (1994): Hydraulic conductivity estimation for soils with heterogeneous pore structure. Water Resources Research, *30*: 211–223.

Ersahin S., Papendick R.I., Smith J.L., Keller C.K., Manoranjan V.S. (2002): Macropore transport of bromide as influenced by soil structure differences. Geoderma, *108*: 207–223.

Flury M. (1996): Experimental evidence of transport of pesticides through field soils. A review. Journal of Environmental Quality, *25*: 558–566.

Flury M., Fluhler H., Jury W.A., Leuenberger J. (1994): Susceptibility of soils to preferential flow of water: A field study. Water Resources Research, *30*: 1945–1954.

Gerke H.H., van Genuchten M.T. (1993): A dual-porosity model for simulating the preferential movement of water and solutes in structured porous media. Water Resources Research, *29*: 305–319.

Gerke H.H., van Genuchten M.T. (1993): Evaluation of a first-order water transfer term for variably saturated dual-porosity flow models. Water Resources Research, *29*: 1225–1238.

Gottesburen B., Aden K., Barlund I., Brown C., Dust M., Gorlitz G., Jarvis N.J., Rekolainen S., Schafer H. (2000): Comparison of the pesticide leaching models: Results using the Weiherbach dataset. Agricultural Water Management, *44*: 153–181.

Hatfield M.W. (1988): Water and anion movement in a typic Hapludult. [PhD Thesis.] Clemson University, USA.

Hutson J.L., Wagenet R.J. (1995): Multi-region water flow and chemical transport in heterogeneous soils. In: Walker A. et al. (eds.): Theory and applications. Pesticide movement to water. Proceedings BCPC Symposium, Monography 62, Warwick University, Coventry, UK: 171–180.

Jabro J.D., Jemison J.M., Fox R.H., Fritton D.D. (1994): Predicting bromide leaching under field conditions using SLIM and MACRO. Soil Science, *157*: 215–223.

Jarvis N.J. (1995): Simulation of soil water dynamics and herbicide persistence in a silt loam soil using the MACRO model. Ecological Modeling, *81*: 97–109.

Jarvis N.J., Bergstrom L., Dik P.E. (1991b): Modeling water and solute transport in macroporous soil. II. Chloride breakthrough under non-steady flow. Soil Science, *42*: 71–81.

Jarvis N.J., Brown C.D., Granitza E. (2000): Sources of error in model predictions of pesticide leaching: a case study using the MACRO model. Agricultural Water Management, *44*: 247–262.

Jarvis N.J., Johnsson P.E., Dik P.E., Messing I. (1991a): Modeling water and solute transport in macroporous soil. I. Model description and sensitivity analysis. Soil Science, *42*: 59–70.

Jarvis N.J., Larsson M.H. (1998): The MACRO model (Version 4.1) – Technical description. http://130.238.110.134:80/bgf/Macrohtm/macro.htm, Department of Soil Sciences, Swedish University of Agricultural Sciences, Uppsala.

Jarvis N.J., Stahli M., Bergstrom L.F., Johnson H. (1994): Simulation of dichlorprop and bentazon leaching in soils of contrasting texture using the MACRO model. Journal of Environmental Science and Health, *A29*: 1255–1277.

Jarvis N.J., Villholth K.G., Ulen B. (1999): Modeling particle mobilization and leaching in macroporous soil. European Journal of Soil Science, *50*: 621–632.

Larsson M.H., Jarvis N.J. (1999a): A dual-porosity model to quantify macropore flow effects on nitrate leaching. Journal of Environmental Quality, *28*: 1298–1307.

Larsson M.H., Jarvis N.J. (1999b): Evaluation of a dual-porosity model to predict field-scale solute transport in a macroporous soil. Journal of Hydrology, *215*: 153–171.

Loague K., Green R.E. (1991): Statistical and graphical methods for evaluating solute transport models: overview and application. Journal of Control Hydrology, *7*: 51–73.

Mohanty B.P., Bowman R.S., Hendricks J.M.H., van Genuchten M.Th. (1997): New piecewise-continuous functions for modeling preferential flow in an intermittent-flood irrigated field. Water Resources Research, *33*: 2049–2063.

Mualem Y. (1976): A new model for predicting the hydraulic conductivity of unsaturated porous media. Water Resources Research, *12*: 513–522.

Nelson P.A. (1990): Solute movement and root distribution as affected by soil structure. [PhD Thesis.] Clemson University, USA.

Quisenberry V.L., Philips R.E. (1976): Percolation of surface applied water in the field. Soil Science Society of American Proceedings, *40*: 484–489.

Quisenberry V.L., Phillips R.E., Zeleznik J.M. (1994): Spatial distribution of water and chloride macropore flow in a well-structured soil. Soil Science Society of American Journal, *58*: 1294–1300.

Richards L.A. (1931): Capillary conduction of liquids through porous mediums. Physics, *1*: 318–333.

Romkens M.J.M., Phillips R.E., Selim H.M., Whisler F.D. (1985): Physical characteristics of soils in the southern region: Vicksburg, Memphis, and Maury series. Southern Cooperating Bulletin, No. 266. MS. Agricultural Experimental Station, Starkville.

Roulier S., Jarvis N.J. (2003a): Analysis of inverse procedures for estimating parameters controlling macropore flow and solute transport in the dual-permeability model MACRO. Vadose Zone Journal, *2*: 349–357.

Roulier S., Jarvis N.J. (2003b): Modeling macropore flow effects on pesticide leaching: Inverse parameter estimation using microlysimeters. Journal of Environmental Quality, *32*: 2341–2353.

Sadeghi A.M., Isensee A.R., Shirmohammadi A. (2000): Influence of soil texture and tillage on herbicide transport. Chemosphere, *41*: 1327–1332.

Saxena R.K., Jarvis N.J., Bergstrom L. (1994): Interpreting non-steady state tracer breakthrough experiments in sand and clay soil using a dual-porosity model. Journal of Hydrology, *162*: 279–298.

Skopp J., Gardner W.R., Tyler E.J. (1981): Solute movement in structured soils: Two-region model with small interaction. Soil Science Society of American Journal, *45*: 837–842.

Thomas G.W., Swoboda A.R. (1970): Anion exclusion effects on chloride movement in soils. Soil Science, *110*: 163–166.

van Genuchten M.Th., Cleary R.W. (1976): Movement of solutes in soil. In: Bolt G.H. (ed.): Soil chemistry. Part B. Physico-chemical models. Elsevier, New York: 349–386.

van Genuchten M.Th., Dalton F.N. (1986): Models for simulating salt movement in aggregated field soils. Geoderma, *38*: 165–183.

Villholth K.G., Jensen K.H. (1998): Flow and transport processes in a macroporous subsurface-drained glacial till soil. II: Model analysis. Journal of Hydrology, *207*: 121–135.

Zurmuhl T., Durner W. (1998): Determinations of parameters for bimodal hydraulic functions by inverse modeling. Soil Science Society of American Journal, *62*: 874–880.

Received on May 3, 2004

ABSTRAKT

Hodnocení modelu MACRO pro krátkodobou simulaci transportu vody a roztoku u půdy Maury silt loam

V posledních třiceti letech je modelování preferenčního proudění v centru pozornosti řady akademických disciplín na celém světě a pomáhá omezit kontaminaci podzemních vod. Model duální pórovitosti MACRO byl hodnocen pro krátkodobou simulaci (kratší než dva dny) proudění vody a transportu roztoku (chloridu) půdním profilem dobře strukturované půdy Maury silt loam na šesti plochách. Proudění vody v mikropórech je počítáno Richardsovou rovnicí a v makropórech je uvažováno jednoduché gravitační proudění. Transport roztoku v mikrofórech je počítán konvekčně-disperzní rovnicí (CDE) se zanedbáním disperze a difúze v rovnici CDE pro transport roztoku v makropórech. Aplikovaná voda a chlorid dosáhly dna profilu ve studii druhé a třetí během dvou a jedné hodiny po zahájení aplikace, což u experimentální půdy jednoznačně ukazuje na proudění v makropórech. Na základě statistických kritérií je zřejmé, že model dobře simuloval proudění vody a roztoku v čase a hloubce v profilu. Průměrné hodnoty tří statistických parametrů (koeficient reziduální hmotnosti, modelová efektivnost a korelační koeficient) pro transport vody a chloridu byly –0,0014; 0,791; 0.903 a 0,0333; 0,923; 0,956. Předcházející studie ukázaly, že model nemůže simulovat proudění a transport dostatečně dobře při použití konceptu jedné domény. Při použití dvoudoménového konceptu (mikropóry a makropóry) byly nejdůležitějšími parametry, které řídí proudění a transport mezi oběma doménami, efektivní délka difúzní dráhy, hydraulická vodivost na okraji a potenciál půdní vody na okraji. Efektivní délka difúzní dráhy charakterizuje u půdy Maury silt loam stav vývoje půdní struktury v závislosti na hloubce.

Klíčová slova: MACRO; proudění v makropórech; modelování; transport roztoků; strukturní půda; dvoudoménový

Corresponding author:

Hasan Merdun, Kahramanmaraş Sütçü Imam University, Faculty of Agriculture, Department of Agricultural Engineering, 46060 Kahramanmaraş, Turkey
phone: 90 (344) 223 7666/433, fax: 90 (344) 223 0048, e-mail: merdun@ksu.edu.tr